Jundishapur J Nat Pharm Prod. 2026 August; 21(3): e173185 https://doi.org/10.5812/jjnpp-173185

Published Online: 2026 July 18 **Research Article**

Eicosapentaenoic Acid as a Bioactive Liquid Lipid in Methotrexate-Loaded Nanostructured Lipid Carriers

Eskandar Moghimipour [1,2], Anayatollah Salimi [1,2,*], Somayeh Handali [3], Dian Dayer [4], Alireza Malayeri [5], Hossein Heidari Kaydan [1], Ali Javadiyeh [1,**]

[1] Department of Pharmaceutics, Faculty of Pharmacy, Ahvaz Jundishapur University of Medical Sciences, Ahvaz, Iran
[2] Nanotechnology Research Center, Ahvaz Jundishapur University of Medical Sciences, Ahvaz, Iran
[3] Medical Biomaterials Research Center (MBRC), Tehran University of Medical Sciences, Tehran, Iran
[4] Cellular and Molecular Research Center, Medical Basic Sciences Research Institute, Ahvaz Jundishapur University of Medical Sciences, Ahvaz, Iran.
[5] Department of Pharmacology, School of Pharmacy, Ahvaz Jundishapur University of Medical Sciences, Ahvaz, Iran

[*] ***Corresponding Author:*** Department of Pharmaceutics, faculty of Pharmacy, Ahvaz Jundishapur University of Medical Science, Ahvaz, Iran. Email: anayatsalimi2003@yahoo.com
[**] ***Corresponding Author:*** Department of Pharmaceutics, Faculty of Pharmacy, Ahvaz Jundishapur University of Medical Sciences, Ahvaz, Iran. Email: alijavadiyeh2025@gmail.com

Received: 29 June, 2026; **Revised:** 11 July, 2026; **Accepted:** 12 July, 2026

Abstract

Background: Nanostructured lipid carriers (NLCs) are promising vehicles for the topical delivery of poorly permeable drugs such as methotrexate (MTX). In conventional NLCs, the liquid lipid serves primarily as a structural component, whereas incorporating a bioactive natural liquid lipid may provide additional formulation benefits for the resulting carrier.

Objectives: This study aimed to design and physicochemically characterize MTX-loaded NLCs using eicosapentaenoic acid (EPA), a natural omega-3 fatty acid, as a bioactive liquid lipid, and to identify an optimal formulation through a systematic two-level formulation design.

Methods: Eight formulations were prepared by hot emulsification followed by sonication, with varying amounts of solid lipid (stearic acid), liquid lipid (EPA), and surfactant (soya lecithin). The MTX assay was validated by reversed-phase high-performance liquid chromatography (HPLC) for linearity, limit of detection (LOD), limit of quantification (LOQ), precision, selectivity, and matrix-matched recovery. The formulations were characterized in terms of particle size, polydispersity index (PDI), zeta potential, entrapment efficiency (EE%), drug loading (DL%), and in vitro release. The release kinetics of the optimal formulation were evaluated using four models (zero-order, first-order, Higuchi, and Korsmeyer-Peppas), and physical stability was monitored for three months.

Results: The HPLC method was linear over 1 - 20 μg/mL (R^2 = 0.9981), with LOD and LOQ of 1.56 and 4.72 μg/mL, respectively, and precision of RSD ≤ 2%. Particle size ranged from 88.92 to 160.7 nm, and PDI ranged from 0.252 to 0.405. The optimal formulation (F5; stearic acid 200 mg, EPA 20 mg, lecithin 40 mg) showed a particle size of 88.92 nm, a PDI of 0.284, a zeta potential of −18.5 mV, an EE% of 88.40%, and a DL% of 7.89%. Its 24 h cumulative release reached 88.03%; among the tested models, the release best fit the Korsmeyer-Peppas (R^2 = 0.987; n = 1.12) and first-order (R^2 = 0.977) models, indicating a coupled diffusion–relaxation mechanism. All formulations remained physically stable over three months.

Conclusions: EPA can serve as a bioactive liquid lipid in NLCs, producing nanoscale carriers with high entrapment, adequate drug loading, and sustained release. These findings provide a robust physicochemical basis for topical MTX carriers; however, biological and skin-delivery validation is required before any therapeutic benefit of EPA can be claimed.

Keywords: Nanostructured Lipid Carriers, Eicosapentaenoic Acid (EPA), Methotrexate, Physicochemical Characterization, Sustained Release

1. Background

How to Cite: Moghimipour E, Salimi A, Handali S, Dayer D, Malayeri A, et al. Eicosapentaenoic Acid as a Bioactive Liquid Lipid in Methotrexate-Loaded Nanostructured Lipid Carriers. Jundishapur J Nat Pharm Prod. 2026;21(3):e173185. doi: https://doi.org/10.5812/jjnpp-173185

Psoriasis is a chronic, immune-mediated inflammatory skin disease characterized by hyperproliferation and aberrant differentiation of keratinocytes, in which the interleukin (IL)-23/Th17/IL-17 axis plays a central pathogenic role (1-4). Methotrexate (MTX), a folate antagonist with antiproliferative and anti-inflammatory properties, remains a cornerstone of systemic therapy for moderate-to-severe disease (5-7). However, systemic MTX is associated with hepatotoxicity, gastrointestinal disturbances, and haematological adverse effects; given its well-documented hepatotoxic liability, localizing the drug within the skin through topical delivery is an attractive strategy to limit systemic exposure while maintaining local efficacy (5-6, 8). Nevertheless, the poor permeability of MTX across the stratum corneum substantially limits this approach (9-12).

Lipid-based nanocarriers have emerged as effective platforms for cutaneous drug delivery. Nanostructured lipid carriers (NLCs) represent a second generation of lipid nanoparticles in which a solid lipid is deliberately blended with a liquid lipid (13-16). The resulting matrix is less ordered than that of purely solid systems, and the structural imperfections it contains create additional space for drug molecules while limiting drug expulsion as the lipid recrystallizes during storage (13, 15). Because the ratio and nature of the solid and liquid lipids critically govern the emulsification behaviour and internal structure of such carriers, careful selection of the liquid-lipid phase is central to formulation performance (17). Compared with solid lipid nanoparticles, this architecture typically affords a higher payload, more controlled release, and improved contact with the skin surface (18-21).

Lipid nanocarriers loaded with MTX or other antipsoriatic agents have been investigated for topical use and have generally improved cutaneous drug deposition while reducing systemic exposure (22-29). In most reported NLCs, however, the liquid lipid is a pharmacologically inert oil whose role is purely structural. Replacing this inert component with a bioactive natural lipid could, in principle, add formulation value beyond a purely structural function. Eicosapentaenoic acid (EPA), a long-chain omega-3 polyunsaturated fatty acid abundant in marine sources, is a natural compound with well-documented anti-inflammatory and antioxidant activities (30-32). Beyond these biological effects, the liquid state and amphiphilic character of EPA make it a plausible candidate for use as the liquid-lipid phase of an NLC, where it may enhance matrix imperfection while contributing additional formulation potential (33).

Despite growing interest in lipid nanocarriers for dermal delivery, the use of a bioactive omega-3 fatty acid as the structural liquid lipid in an MTX-loaded NLC has not been systematically characterized. Establishing how EPA influences particle size, entrapment, and release behaviour in such carriers is a prerequisite for their rational development.

2. Objectives

This study was designed to formulate and physicochemically characterize MTX-loaded NLCs using EPA as a bioactive natural liquid lipid. Specifically, the objectives were to validate a reversed-phase HPLC method for MTX quantification; to prepare a series of formulations using a systematic two-level formulation design involving a solid lipid, a liquid lipid, and a surfactant; to characterize the resulting carriers in terms of particle size, PDI, zeta potential, EE%, and DL%; to evaluate in vitro release and its kinetic behaviour using multiple models; and to assess the physical stability of the formulations over three months.

3. Methods

3.1. Materials

Methotrexate (purity ≥ 99%) and stearic acid (analytical grade) were purchased from Merck (Darmstadt, Germany). Eicosapentaenoic acid (EPA; purity ≥ 98%) was obtained from [INSERT SUPPLIER, city, country]. Soya lecithin (pharmaceutical grade) and sodium glycolate were obtained from [INSERT SUPPLIER, city, country]. Acetonitrile and all other solvents were of HPLC grade; all remaining reagents were of analytical grade. Double-distilled water was used throughout.

3.2. HPLC Method and Validation

Methotrexate was quantified using a Knauer HPLC system (Knauer, Berlin, Germany) equipped with a photodiode-array detector. Separation was performed on a C18 column (250 × 4.0 mm, 5 μm) using a mobile phase of 0.05 M phosphate buffer–acetonitrile (86:14, v/v), adjusted to pH 3.9 and delivered at 1.0 mL/min. The injection volume was 20 μL, the column temperature was 30 °C, and detection was performed at 303 nm. Calibration standards were prepared at 1, 2.5, 5, and 20 μg/mL, and linearity was assessed by least-squares regression of peak area versus concentration.

The method was validated according to ICH Q2(R1). The limit of detection (LOD) and limit of quantification (LOQ) were calculated from the residual standard deviation of the regression line (σ) and its slope (S) as

3.3σ/S and 10σ/S, respectively. Intra-day and inter-day precision were evaluated at three concentrations across the calibration range and expressed as the relative standard deviation (RSD), with RSD ≤ 2% predefined as the acceptance criterion. Selectivity was verified by injecting a drug-free (blank) lipid matrix prepared identically to the formulations but without the drug, confirming the absence of interfering peaks at the MTX retention time. Accuracy was assessed using a matrix-matched recovery study in which known amounts of MTX were spiked into the blank lipid matrix at low, medium, and high levels and quantified against the calibration line. System suitability was verified before each run by assessing the reproducibility of the retention time and peak area of the MTX standard.

3.3. Experimental Arrangement and Preparation of NLCs

To examine the influence of formulation variables on carrier properties, a two-level formulation arrangement with three independent factors was adopted: the amount of solid lipid (stearic acid, 200 mg [coded –1] / 600 mg [coded +1]), the amount of liquid lipid (EPA, 20 mg [–1] / 60 mg [+1]), and the amount of surfactant (soya lecithin, 40 mg [–1] / 60 mg [+1]). Factor levels were coded as –1 (low) and +1 (high). Sodium glycolate was not treated as an independent factor; it served as a nested, dependent co-stabilizer, with its amount fixed relative to the surfactant content (50% or 25% of the soya-lecithin mass) to preserve emulsion integrity across compositions. Eight formulations (F1–F8) were prepared accordingly, while the MTX content was held constant at 25 mg (Table 1).

NLCs were prepared by hot emulsification followed by sonication. Briefly, the weighed amounts of stearic acid and EPA were melted in a water bath at approximately 70 °C (a few degrees above the melting point of the solid lipid) to obtain a homogeneous lipid phase; lecithin and then the fixed amount of MTX were dispersed in the molten phase. The aqueous phase was prepared by dissolving sodium glycolate in double-distilled water and heating to the same temperature to minimize the interphase temperature difference. The aqueous phase was then added to the lipid phase and homogenized at 12,000 rpm for 10 min to form a coarse emulsion, which was subsequently probe-sonicated for 5 min (60% amplitude, 0.6 cycle) to obtain a nanoscale dispersion. The dispersion was allowed to cool to room temperature.

3.4. Particle Size, PDI, and Zeta Potential

The mean particle size and PDI were determined by dynamic light scattering, and the zeta potential was measured by electrophoretic light scattering; both are widely used as critical quality attributes governing the stability and cutaneous behaviour of lipid nanocarriers (34-35). All measurements were performed in triplicate and are reported as mean ± standard deviation (SD).

3.5. Entrapment Efficiency and Drug Loading

Entrapment efficiency (EE%) was determined indirectly. A 2-mL aliquot of the NLC dispersion was centrifuged at 20,000 rpm for 30 min to sediment the nanoparticles; the supernatant containing free drug was separated, diluted, and assayed by HPLC. EE% and DL% were calculated using Equations 1 and 2, respectively. All measurements were performed in triplicate.

$$\mathrm{EE}\,(\%) = \left[\frac{\frac{W_{\text{total drug})}}{W_{\text{free drug}}}}{W_{\text{total}}\,\text{drug}}\right] \times 100$$

$$\mathrm{DL}\,(\%) = \left[\frac{W_{\text{entrapped drug}}}{\left(W_{\text{total lipid}} + W_{\text{entrapped drug}}\right)}\right] \times 100$$

3.6. In Vitro Release and Kinetic Modeling

In vitro release of MTX was evaluated using vertical Franz diffusion cells. The receptor compartment was filled with phosphate-buffered saline (PBS, pH 7.4) and maintained at 37 ± 0.5 °C under continuous magnetic stirring; the medium volume was selected to maintain sink conditions for MTX throughout the study. The donor and receptor compartments were separated by a pre-hydrated regenerated-cellulose dialysis membrane (molecular-weight cut-off 12,000 Da), selected as an inert, reproducible diffusion barrier that isolates drug release from the carrier from skin-permeation variables. At 0.5, 1, 2, 3, 4, 5, 6, 12, and 24 h, 1 mL was withdrawn from the receptor compartment and immediately replaced with an equal volume of fresh pre-warmed medium. The withdrawn samples were assayed using the validated HPLC method, and the cumulative percentage released was plotted versus time. Each experiment was performed in triplicate. To elucidate the release mechanism of the optimal formulation, the cumulative release data were fitted to four kinetic models—zero-order, first-order, Higuchi, and Korsmeyer-Peppas (36-38)—and the goodness of fit was assessed by

Table 1. Composition of the Prepared Formulations (F1 - F8) [a]

Formulations	MTX (mg)	Stearic acid (mg)	EPA (mg)	Soya lecithin (mg)	Sodium glycolate (mg)
F1	25	300	30	60	30
F2	25	300	30	60	15
F3	25	600	60	60	30
F4	25	600	60	60	15
F5	25	200	20	40	20
F6	25	200	20	40	10
F7	25	400	40	40	20
F8	25	400	40	40	10

[a] Coded levels — stearic acid: 200 mg (−1)/600 mg (+1); EPA: 20 mg (−1)/60 mg (+1); soya lecithin: 40 mg (−1)/60 mg (+1). Sodium glycolate is a nested co-stabilizer fixed at 50% or 25% of the surfactant mass and is not an independent factor. The amount of MTX was held constant across all formulations. Abbreviations: MTX, methotrexate; EPA, eicosapentaenoic acid.

the coefficient of determination (R^2). For the Korsmeyer-Peppas model, the release exponent (n) was used to interpret the transport mechanism. The Franz diffusion cell employed has been validated as a standard in vitro permeation system (39).

3.7. Surface Morphology

The surface morphology of the optimal formulation was examined by atomic force microscopy (AFM) following appropriate sample preparation, and both two-dimensional (error-signal) and three-dimensional (topography) images were acquired.

3.8. Physical Stability

The physical stability of all formulations was evaluated over three months of refrigerated storage by monitoring particle size, PDI, and zeta potential at 0, 1, and 3 months.

3.9. Statistical Analysis

Data are expressed as mean ± SD. Comparisons among groups were performed using analysis of variance (ANOVA), followed by the Tukey post-hoc test. Exact probability values are reported, and a probability value of less than 0.05 was considered statistically significant.

4. Results

4.1. HPLC Method Validation

The calibration curve for MTX was linear over the concentration range of 1 - 20 μg/mL, with the regression equation y = 117.73x − 58.298 and a coefficient of determination (R^2) of 0.9981, indicating excellent linearity across the studied range (Figure 1). From the residual standard deviation of the regression line (σ = 55.59) and its slope (S = 117.73), the LOD and LOQ were calculated as 1.56 μg/mL and 4.72 μg/mL, respectively, confirming that the method was sufficiently sensitive for the studied concentrations. Under the described conditions, MTX eluted as a single, well-defined peak, with a retention time of approximately 5.29 min at 303 nm (Figure 2). Selectivity was confirmed by the absence of interfering peaks from the blank lipid matrix at the MTX retention time, demonstrating that stearic acid, EPA, soya lecithin, and sodium glycolate did not compromise quantification. Intra-day and inter-day precision were within the predefined acceptance limit (RSD ≤ 2%), and the matrix-matched recovery of MTX was within the acceptable range, collectively confirming the accuracy and reliability of the assay for MTX quantification in the lipid matrix.

4.2. Physicochemical Properties of the Formulations

The physicochemical properties of the eight formulations are summarized in Table 2. The mean particle size ranged from 88.92 to 160.7 nm, and the PDI ranged from 0.252 to 0.405, indicating predominantly nanoscale and reasonably homogeneous dispersions. The zeta potential was negative for all formulations (−15.23 to −21.71 mV), consistent with electrostatically stabilized systems. The EE% varied between 73.41% and 88.40%, and the DL% between 2.76% and 7.89%. The highest EE% and DL% were obtained for formulation F5; its encapsulation efficiency was significantly higher than that of F8 ($P < 0.001$), and its particle size was significantly smaller than that of F1 ($P < 0.001$).

4.3. Selection of the Optimal Formulation

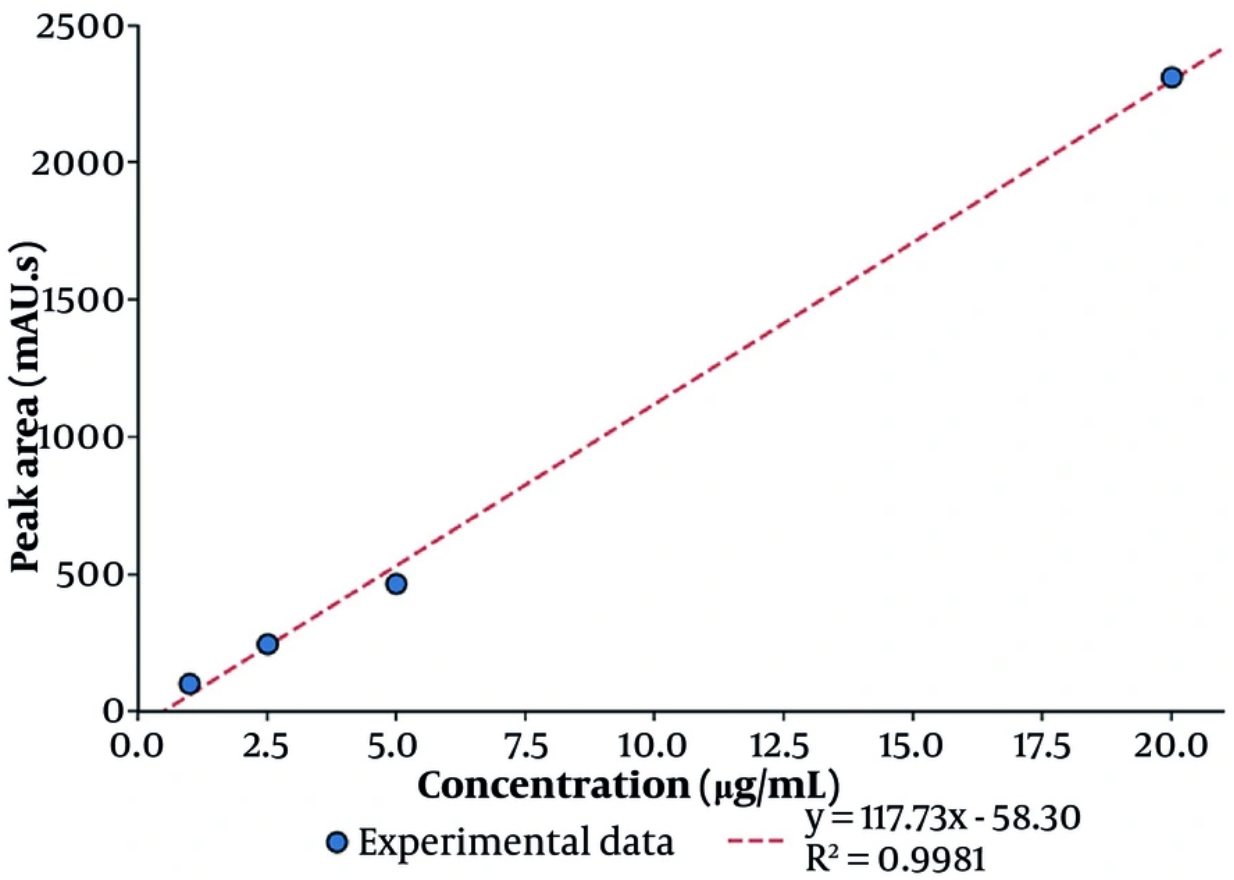

Figure 1. Calibration curve of methotrexate over the range of 1 - 20 µg/mL obtained by the HPLC method (y = 117.73x – 58.298; R^2 = 0.9981).

Optimal formulation selection was based on Derringer's multi-response desirability approach. Each response was transformed into an individual desirability score, with response limits denoted by Y_{min} and Y_{max}. The overall desirability was calculated as a weighted geometric mean with terms including d_1, w_1, d_2, and w_2, with equal weights assigned to all responses. On this basis, formulation F5 — composed of stearic acid (200 mg), EPA (20 mg), lecithin (40 mg), and sodium glycolate (20 mg) — attained the highest overall desirability (D = 0.971) and was selected as the optimal formulation. Although F8 exhibited the highest 24 h cumulative release (90.13%), its lower encapsulation efficiency and larger particle size reduced its overall desirability relative to F5, which provided the most favourable overall balance of small particle size, high EE% and DL%, and adequate sustained release. The principal characteristics of F5 are presented in Table 3.

4.4. In Vitro Release and Release Kinetics

The cumulative release of MTX increased over time for all formulations, and the 24 h cumulative release ranged from 65.46% (F1) to 90.13% (F8). The optimal formulation, F5, exhibited a 24 h cumulative release of 88.03%, reflecting an adequate and sustained release profile (Figure 3). The release data for F5 were fitted to four kinetic models (Table 4). The Korsmeyer-Peppas model yielded the highest coefficient of determination (R^2 = 0.987), closely followed by the first-order model (R^2 = 0.977), whereas the Higuchi and zero-order models yielded R^2 = 0.943 and 0.823, respectively (Figure 4).

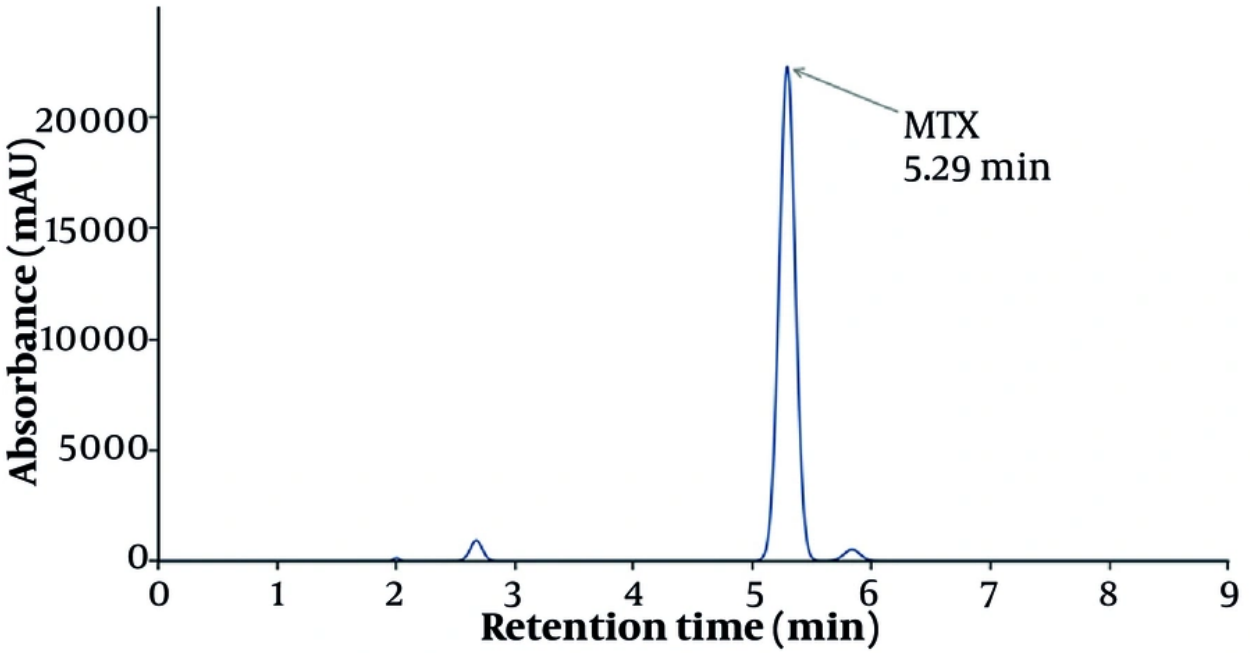

Figure 2. Representative HPLC chromatogram of standard methotrexate at 303 nm, showing a retention time of approximately 5.29 min.

Table 2. Physicochemical Properties of the Prepared Formulations (F1 - F8) [a]

Formulation	Particle size (nm)	PDI	Zeta potential (mV)	EE (%)	DL (%)
F1	160.7 ± 4.2	0.289	−18.0	73.41 ± 0.37	4.37 ± 0.02
F2	110.2 ± 3.1	0.274	−21.46	84.69 ± 1.19	5.22 ± 0.07
F3	102.6 ± 2.9	0.252	−15.23	87.66 ± 0.34	2.92 ± 0.02
F4	116.5 ± 3.4	0.309	−17.18	81.17 ± 0.43	2.76 ± 0.02
F5	88.92 ± 2.1	0.284	−18.5	88.40 ± 0.44	7.89 ± 0.04
F6	103.3 ± 3.8	0.405	−16.86	77.72 ± 0.29	7.20 ± 0.03
F7	92.37 ± 2.7	0.285	−21.71	80.03 ± 0.23	4.00 ± 0.01
F8	121.0 ± 3.9	0.354	−19.3	76.21 ± 0.36	3.89 ± 0.02

[a] Values are expressed as mean ± SD (n = 3). Abbreviations: PDI, polydispersity index; EE%, entrapment efficiency; DL%, drug loading.

Because the first-order and Korsmeyer-Peppas models fitted comparably well, release from the F5 matrix is unlikely to be governed by a single simple mechanism. The Korsmeyer-Peppas diffusion exponent ($n = 1.12$) exceeds unity, indicating an anomalous (Super Case-II) transport regime in which lipid-matrix relaxation and gradual erosion contribute alongside diffusion, rather than purely Fickian diffusion ($n \leq 0.45$). This behaviour is consistent with the semi-solid, imperfect-crystalline architecture of NLCs. Accordingly, while the Higuchi model provides an acceptable description of the diffusional component, the overall release of MTX from the EPA-based matrix is best described as a coupled diffusion–relaxation process; this interpretation is offered cautiously for a single optimized formulation.

4.5. Surface Morphology

Table 3. Characteristics of the Optimal Formulation (F5) [a]

Variables	Value
Particle size (nm)	88.92 ± 2.1
PDI	0.284
Zeta potential (mV)	−18.5
EE (%)	88.40 ± 0.44
DL (%)	7.89 ± 0.04
24 h release (%)	88.03 ± 1.45

[a] Values are expressed as mean ± SD (n = 3).

Table 4. Release Kinetic Parameters for the Optimal Formulation (F5) [a]

Model	Equation	Rate constant	R^2
Zero-order	$Q = k_0 \cdot t$	$k_0 = 3.57\% \cdot h^{-1}$	0.823
First-order	$\ln(100 - Q) = \ln 100 - k_1 \cdot t$	$k_1 = 0.090\ h^{-1}$	0.977
Higuchi	$Q = k_H \cdot \sqrt{t}$	$k_H = 21.92\% \cdot h^{-1/2}$	0.943
Korsmeyer-Peppas	$\log Q = \log k + n \cdot \log t$	n = 1.12; k = 6.92	0.987

[a] Abbreviations: Q, cumulative percentage released; t, time; n, release exponent.

Atomic force microscopy of the optimal formulation revealed predominantly spherical particles with a relatively uniform distribution; both two-dimensional (error-signal) and three-dimensional (topography) images are shown (Figure 5). Minor aggregates observed in the images were attributable to the drying step during sample preparation. Overall, the morphological findings were consistent with the successful formation of lipid nanoparticles.

4.6. Physical Stability

Over three months of refrigerated storage, all formulations exhibited only limited changes: particle size increased marginally (by approximately 5 - 10 nm), the absolute zeta potential decreased slightly, and the PDI remained largely below 0.4. These limited changes indicate the absence of substantial particle aggregation and confirm acceptable physical stability of the carriers. The optimal formulation, F5, maintained satisfactory stability throughout the study period (Table 5).

5. Discussion

The present study demonstrates that eicosapentaenoic acid (EPA), a natural omega-3 fatty acid, can serve as an effective liquid-lipid phase in methotrexate (MTX)-loaded nanostructured lipid carriers, yielding nanoscale carriers that combine a small particle size with high entrapment and a sustained release profile. Among the eight formulations examined, the optimal system (F5) simultaneously achieved the smallest particle size (88.92 nm), the highest entrapment efficiency (88.40%), and the highest drug loading (7.89%), indicating a favourable balance among the solid lipid, liquid lipid, and surfactant. A distinguishing feature of this work is that the liquid lipid was not a pharmacologically inert oil, as is common in conventional NLCs, but a bioactive natural compound, thereby integrating a structural role with additional formulation potential within a single carrier.

The favourable physicochemical profile of the optimal formulation can be rationalized on biophysical grounds. The incorporation of a liquid lipid such as EPA into a solid stearic-acid matrix is expected to disrupt the regular crystalline lattice, yielding a less ordered, more amorphous structure with a greater number of imperfections. These imperfections create additional space to accommodate drug molecules and reduce the tendency of the drug to be expelled as the lipid recrystallizes during storage; together, these effects account for the high entrapment and loading recorded for F5. This interpretation is consistent with the original conception of NLCs as second-generation lipid nanoparticles (13-16).

The encapsulation efficiency of F5 (88.40%) and its sub-100-nm particle size compare favourably with

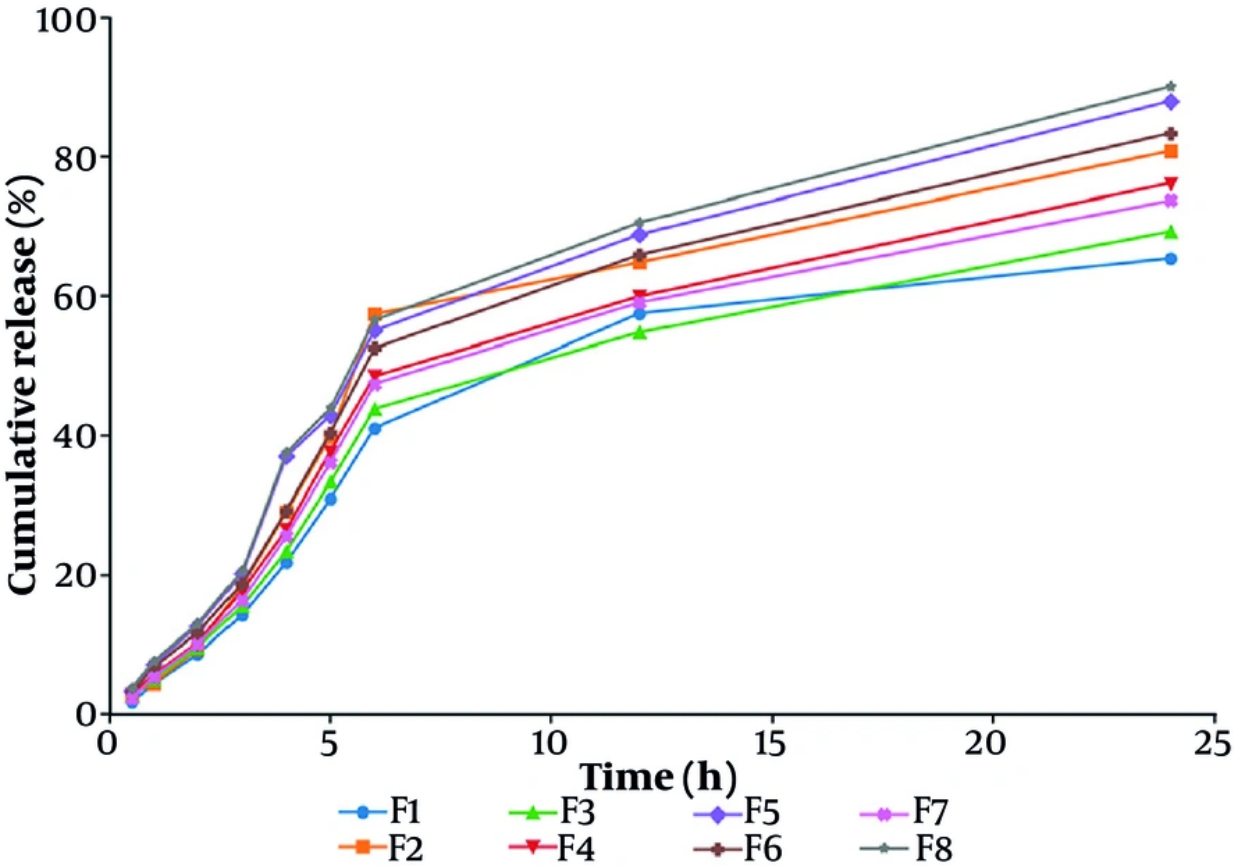

Figure 3. in vitro cumulative release profiles of methotrexate from all formulations (F1–F8) (mean ± SD, n = 3).

previously reported MTX-loaded lipid nanoparticles for topical use, in which entrapment values of ~70 - 90% and particle sizes of ~100 - 250 nm are typical (22-23). Comparable physicochemical characterization strategies have recently been applied to other nanocarrier systems, such as antibiotic-loaded alginate–chitosan nanogels, underscoring the general applicability of the present characterization approach (40). Collectively, these comparisons indicate that EPA did not appear to compromise efficient drug encapsulation.

The particle size of all formulations remained below approximately 161 nm, and that of the optimal formulation was well under 100 nm; particle dimensions in this range are generally considered favourable for cutaneous delivery because they promote close contact with the stratum corneum and may facilitate accumulation within skin appendages and intercellular lipid domains (11, 18-21). The polydispersity index of the optimal formulation was 0.284, indicating a reasonably homogeneous population, and the negative zeta potential observed across the series (−15.23 to −21.71 mV) is consistent with electrostatically stabilized dispersions. The preservation of both particle size and zeta potential over three months of refrigerated storage indicates adequate physical stability and the absence of significant aggregation, consistent with the established role of these parameters as critical quality attributes of lipid nanocarriers (34-35, 41).

The relationships between the formulation variables and the measured responses were not strictly monotonic; for example, the largest amounts of solid lipid did not yield the smallest particles or the highest loading, and intermediate compositions frequently outperformed the extremes. This behaviour indicates that carrier properties are governed by the interplay

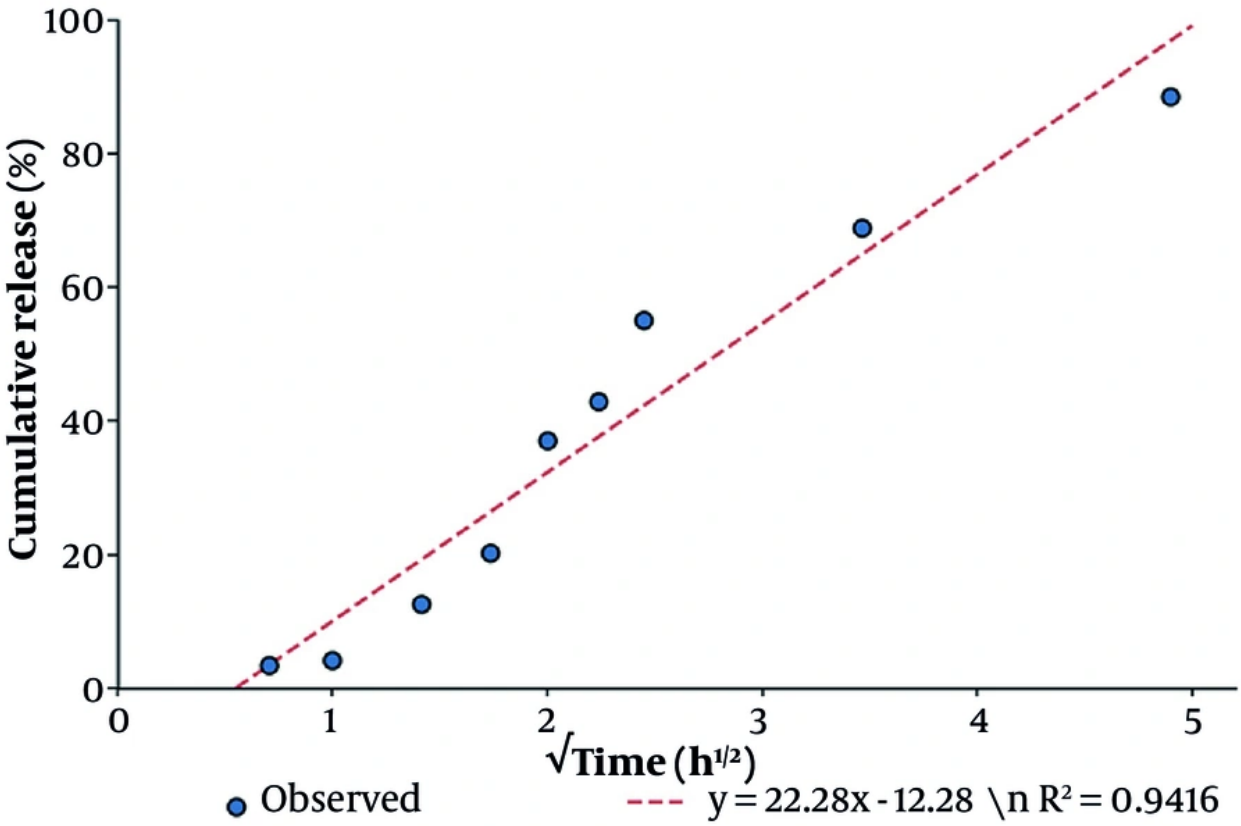

Figure 4. Higuchi model fit for the release of methotrexate from formulation F5 (cumulative percentage released versus the square root of time).

among the solid lipid, the liquid lipid, and the surfactant rather than by any single factor in isolation, underscoring the value of a systematic, multifactor approach to identifying a balanced composition (42). It should be noted, however, that a formal analysis-of-variance decomposition of the main and interaction effects was not undertaken in this phase and is a defined objective of the ongoing optimization study.

The release of MTX from the optimal formulation followed a characteristic biphasic pattern, comprising an initial, relatively rapid phase followed by a slower, sustained phase. The initial phase is attributable to the fraction of drug located at or near the particle surface and within the surfactant layer, whereas the sustained phase reflects the gradual diffusion of drug entrapped within the lipid matrix. Comparison across four kinetic models showed that the first-order and Korsmeyer-Peppas models fitted the data comparably well, and the Korsmeyer-Peppas exponent (n = 1.12) indicated an anomalous (Super Case-II) transport regime rather than purely Fickian diffusion. This finding suggests that lipid-matrix relaxation and gradual erosion contribute to release alongside diffusion, as expected for the imperfect, matrix-type architecture of NLCs. Comparable sustained release has been reported for other MTX-loaded lipid nanoparticles intended for topical use (22-23), and such a profile is desirable for a topical carrier because it can prolong local drug availability while limiting peak concentrations associated with irritation.

Beyond its structural contribution, the selection of EPA as the liquid lipid is conceptually attractive. Unlike the inert oils customarily employed in NLCs, EPA is a bioactive natural compound with well-documented anti-inflammatory and antioxidant activities (30-32). The use of such a lipid as the structural liquid phase therefore raises the possibility of additional value from the carrier matrix itself; however, because no cellular or

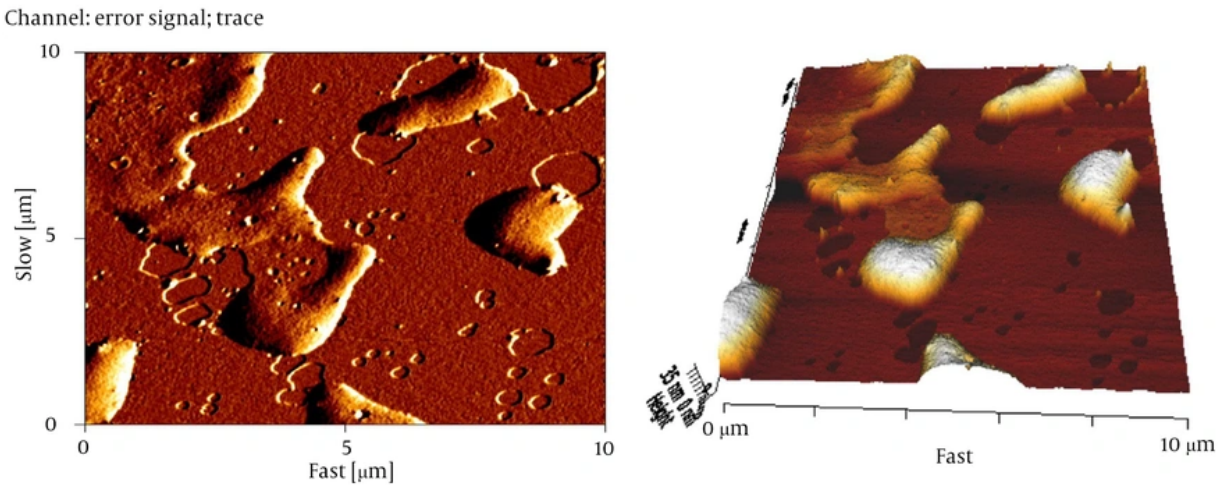

Figure 5. Atomic force microscopy images of the optimal formulation (F5): (a) two-dimensional error-signal image and (b) three-dimensional topography.

Table 5. Particle Size (Nm) of the Formulations During Three Months of Storage [a]

Formulations	0 (mo)	1 (mo)	3 (mo)
F1	160.7 ± 4.2	165.9 ± 4.8	171.0 ± 5.3
F2	110.2 ± 3.1	113.8 ± 3.6	118.4 ± 4.1
F3	102.6 ± 2.9	106.7 ± 3.3	119.09 ± 3.8
F4	116.5 ± 3.4	121.2 ± 3.9	125.8 ± 4.5
F5	88.92 ± 2.1	91.4 ± 2.6	94.8 ± 3.1
F6	103.3 ± 3.8	109.6 ± 4.5	116.9 ± 5.2
F7	92.37 ± 2.7	96.8 ± 3.2	101.5 ± 3.9
F8	121.0 ± 3.9	126.4 ± 4.6	132.2 ± 5.4

[a] Values are expressed as mean ± SD (n = 3).

in vivo experiments were performed in this phase, any therapeutic contribution of EPA remains a hypothesis to be tested. Accordingly, EPA is characterized here strictly as a bioactive liquid lipid with high formulation potential rather than as a demonstrated therapeutic agent. The present study was deliberately confined to the design and physicochemical characterization of these carriers, which constitute the necessary foundation on which subsequent biological evaluation must rest.

Several limitations should be acknowledged. First, the present phase compared eight EPA-based compositions and did not include a conventional (inert-oil) liquid-lipid NLC as a comparator; such a control is planned to isolate the specific contribution of EPA. Second, solid-state and ultrastructural characterization—differential scanning calorimetry (DSC), X-ray diffraction (XRD), Fourier-transform infrared spectroscopy (FTIR), and transmission electron microscopy (TEM)—were beyond the present scope and are identified as important future prospects to confirm the crystallinity, drug–lipid interactions, and internal morphology inferred here. Third, only physical (colloidal) stability was assessed; because EPA is a polyunsaturated fatty acid susceptible to lipid peroxidation and MTX is prone to hydrolysis and photodegradation, chemical and oxidative stability were not quantified, and antioxidant protection together with forced-degradation studies are recommended. Finally, this work is limited to

physicochemical and in vitro characterization: skin permeation, skin retention, cytocompatibility, and anti-inflammatory efficacy were not evaluated; therefore, the results should be interpreted as demonstrating formulation potential rather than therapeutic performance. Biological and skin-delivery validation remains necessary before therapeutic conclusions can be drawn.

In conclusion, EPA can function as a bioactive natural liquid lipid in MTX-loaded NLCs, yielding nanoscale, physically stable carriers with high entrapment, adequate drug loading, and sustained, predominantly diffusion-coupled release. By demonstrating that a bioactive omega-3 fatty acid can replace the inert liquid lipid of a conventional NLC without compromising physicochemical quality, these findings provide a rational basis for the design of topical lipid nanocarriers; however, the therapeutic value of this platform, and any specific contribution of EPA beyond its formulation role, must be confirmed in subsequent cellular and in vivo studies.

Footnotes

AI Use Disclosure: For the purpose of Text Editing, the Claude Was Used To A Moderate Extent For Language Editing Of The Introduction; All Scientific Content And Interpretation Are The Authors' Own. was used Moderate in the Introduction section.

Authors' Contribution: Study concept and design: A. J., A. S., and E. M. Preparation of the formulations and acquisition of data: A. J., H. H. K., and S. H. Analysis and interpretation of data: A. J., H. H. K., A. M., and D. D. Drafting of the manuscript: A. J. and H. H. K. Critical revision of the manuscript for important intellectual content: A. S. and E. M. Study supervision: E. M. All authors read and approved the final manuscript.

Conflict of Interests Statement: The authors declare that they have no conflict of interest.

Data Availability: The datasets generated and analyzed during the current study are available from the corresponding author on reasonable request.

Ethical Approval: The broader Ph.D. thesis project from which this work derives was approved by the Animal Care Ethics Committee of Ahvaz Jundishapur University of Medical Sciences, Ahvaz, Iran (ethics code: IR.AJUMS.AEC.1404.076; https://ethics.research.ac.ir/ProposalCertificateEn.php?id=838304). The present manuscript is restricted to the physicochemical and in vitro characterization phase of the formulations and reports no experiments involving animals or animal-derived samples.

Funding/Support: This article was extracted from the Ph.D. thesis of Ali Javadiyeh at Ahvaz Jundishapur University of Medical Sciences, Ahvaz, Iran, which financially supported the study (grant number N-0419).

References

1. Boehncke WH, Schön MP. Psoriasis. *Lancet*. 2015;**386**(9997):983-94. [PubMed ID: 26025581]. https://doi.org/10.1016/S0140-6736(14)61909-7.
2. Griffiths CEM, Armstrong AW, Gudjonsson JE, Barker JNWN. Psoriasis. *Lancet*. 2021;**397**(10281):1301-1315. [PubMed ID: 33812489]. https://doi.org/10.1016/S0140-6736(20)32549-6.
3. Rendon A, Schäkel K. Psoriasis pathogenesis and treatment. *Int J Mol Sci*. 2019;**20**(6):1475. [PubMed ID: 30909615]. [PubMed Central ID: PMC6471628]. https://doi.org/10.3390/ijms20061475.
4. Hawkes JE, Yan BY, Chan TC, Krueger JG. Discovery of the IL-23/IL-17 signaling pathway and the treatment of psoriasis. *J Immunol*. 2018;**201**(6):1605-13. [PubMed ID: 30181299]. [PubMed Central ID: PMC6129988]. https://doi.org/10.4049/jimmunol.1800013.
5. Shen S, O'Brien T, Yap LM, Prince HM, McCormack CJ. The use of methotrexate in dermatology: a review. *Australas J Dermatol*. 2012;**53**(1):1-18. [PubMed ID: 22309324]. https://doi.org/10.1111/j.1440-0960.2011.00839.x.
6. Bedoui Y, Guillot X, Sélambarom J, Guiraud P, Giry C, Jaffar-Bandjee MC, et al. Methotrexate an old drug with new tricks. *Int J Mol Sci*. 2019;**20**(20):5023. [PubMed ID: 31658782]. [PubMed Central ID: PMC6834162]. https://doi.org/10.3390/ijms20205023.
7. Qiao L, Hu J, Ou D, Liu M, Shi X, Li X, et al. Comparison of the efficacy and safety of methotrexate injection and methotrexate tablets in active RA. *Rheumatology (Oxford)*. 2025;**64**(6):3426-3433. [PubMed ID: 39918971]. https://doi.org/10.1093/rheumatology/keaf054.
8. Heidari MA, Khalili H, Goudarzi M, Nesari A, Ahangarpour A, Bahreiny SS. Alleviation of Liver Dysfunction, Oxidative Stress and Inflammation Underlies the Protective Effect of Arbutin in Methotrexate-Induced Hepatotoxicity: An In-Depth Biochemical and Histopathological Insights. *Jundishapur J Nat Pharm Prod*. 2026;**21**(1). e167007. https://doi.org/10.5812/jjnpp-167007.
9. Alkilani AZ, Nasereddin J, Hamed R, Nimrawi S, Hussein G, Abo-Zour H, et al. Transdermal drug delivery: innovative pharmaceutical developments. *Pharmaceutics*. 2022;**14**(6):1152. [PubMed ID: 35745725]. [PubMed Central ID: PMC9231212]. https://doi.org/10.3390/pharmaceutics14061152.
10. Pradhan M, Singh D, Singh MR. Novel colloidal carriers for psoriasis: current issues, mechanistic insight and novel delivery approaches. *J Control Release*. 2013;**170**(3):380-95. [PubMed ID: 23770117]. https://doi.org/10.1016/j.jconrel.2013.05.020.
11. Sala M, Diab R, Elaissari A, Fessi H. Lipid nanocarriers as skin drug delivery systems: Properties, mechanisms of skin interactions and medical applications. *Int J Pharm*. 2018;**535**(1 - 2):1-17. [PubMed ID: 29111097]. https://doi.org/10.1016/j.ijpharm.2017.10.046.
12. Hua S. Lipid-based nano-delivery systems for skin delivery of drugs and bioactives. *Front Pharmacol*. 2015;**6**:219. [PubMed ID: 26483690]. [PubMed Central ID: PMC4588690]. https://doi.org/10.3389/fphar.2015.00219.
13. Chauhan I, Yasir M, Verma M, Singh AP. Nanostructured lipid carriers: a groundbreaking approach for transdermal drug delivery. *Adv Pharm Bull*. 2020;**10**(2):150-65. [PubMed ID: 32373485]. [PubMed Central ID: PMC7191226]. https://doi.org/10.34172/apb.2020.021.

14. Fang CL, Al-Suwayeh SA, Fang JY. Nanostructured lipid carriers (NLCs) for drug delivery and targeting. *Recent Pat Nanotechnol*. 2020;**14**(1):1-15. https://doi.org/10.2174/1872210513666190809113046.
15. Duong VA, Nguyen TTL, Maeng HJ. Preparation of solid lipid nanoparticles and nanostructured lipid carriers for drug delivery. *Molecules*. 2020;**25**(20):4781. [PubMed ID: 33081021]. [PubMed Central ID: PMC7587569]. https://doi.org/10.3390/molecules25204781.
16. Naseri N, Valizadeh H, Zakeri-Milani P. Solid lipid nanoparticles and nanostructured lipid carriers: structure, preparation and application. *Adv Pharm Bull*. 2015;**5**(3):305-13. [PubMed ID: 26504751]. [PubMed Central ID: PMC4616893]. https://doi.org/10.15171/apb.2015.043.
17. Hasan N, S Bakhsh R, H Shabakh A, H. Aldhahri D, Y. Dakkak M, S. AL-Harbi M, et al. Characterization of Emulsification Profiles of Developed Lipid Formulation for the Oral Delivery of Poorly Water-Soluble Drugs. *J Rep Pharm Sci*. 2026;**14**(1). e168970. https://doi.org/10.5812/jrps-168970.
18. Gomaa E, Fathi HA, Eissa NG, Elsabahy M. Methods for preparation of nanostructured lipid carriers. *Methods*. 2022;**199**:3-8. [PubMed ID: 33992771]. https://doi.org/10.1016/j.ymeth.2021.05.003.
19. Chauhan MK, Sharma PK. Optimization and characterization of rivastigmine nanolipid carrier loaded transdermal patches for the treatment of dementia. *Chem Phys Lipids*. 2019;**224**. 104794. [PubMed ID: 31361985]. https://doi.org/10.1016/j.chemphyslip.2019.104794.
20. Khosa A, Reddi S, Saha RN. Nanostructured lipid carriers for site-specific drug delivery. *Biomed Pharmacother*. 2018;**103**:598-613. [PubMed ID: 29677547]. https://doi.org/10.1016/j.biopha.2018.04.055.
21. Beloqui A, Solinís MÁ, Rodríguez-Gascón A, Almeida AJ, Préat V. Nanostructured lipid carriers: promising drug delivery systems for future clinics. *Nanomedicine*. 2016;**12**(1):143-61. [PubMed ID: 26410277]. https://doi.org/10.1016/j.nano.2015.09.004.
22. Ferreira M, Chaves LL, Lima SAC, Reis S. Optimization of nanostructured lipid carriers loaded with methotrexate: a tool for inflammatory and cancer therapy. *Int J Pharm*. 2015;**492**(1 - 2):65-72. [PubMed ID: 26169145]. https://doi.org/10.1016/j.ijpharm.2015.07.013.
23. Ferreira M, Silva E, Barreiros L, Segundo MA, Costa Lima SA, Reis S. Methotrexate loaded lipid nanoparticles for topical management of skin-related diseases. *Int J Pharm*. 2016;**512**(1):14-21. [PubMed ID: 27530292]. https://doi.org/10.1016/j.ijpharm.2016.08.008.
24. Lin YK, Al-Suwayeh SA, Leu YL, Shen FM, Fang JY. Squalene-containing nanostructured lipid carriers promote percutaneous absorption. *Pharm Res*. 2013;**30**(4):1163-75. [PubMed ID: 23229860]. https://doi.org/10.1007/s11095-012-0951-x.
25. Avasatthi V, Pawar H, Dora CP, Bansod P, Gill MS, Suresh S. A novel nanogel formulation of methotrexate for topical treatment of psoriasis. *Pharm Dev Technol*. 2016;**21**(5):554-62. [PubMed ID: 26024238]. https://doi.org/10.3109/10837450.2015.1026605.
26. Rapalli VK, Singhvi G, Dubey SK, Gupta G, Chellappan DK, Dua K. Emerging landscape in psoriasis management: from topical application to targeting biomolecules. *Biomed Pharmacother*. 2018;**106**:707-13. [PubMed ID: 29990862]. https://doi.org/10.1016/j.biopha.2018.06.136.
27. Pradhan M, Alexander A, Singh MR, Singh D, Saraf S, Saraf S, et al. Understanding the prospective of nano-formulations towards the treatment of psoriasis. *Biomed Pharmacother*. 2018;**107**:447-63. [PubMed ID: 30103117]. https://doi.org/10.1016/j.biopha.2018.07.156.
28. Mohd Nordin UU, Ahmad N, Salim N, Mohd Yusof NS. Lipid-based nanoparticles for psoriasis treatment: a review on conventional treatments, recent works, and future prospects. RSC Adv. 2021 Sep 1;11(46):29080 - 29101. *Erratum in: RSC Adv*. 2022;**11**(46):29080-29101. [PubMed ID: 35478537]. [PubMed Central ID: PMC9038133]. https://doi.org/10.1039/d1ra06087b.
29. Sahu S, Katiyar SS, Kushwah V, Jain S. Active natural oil-based nanoemulsion containing tacrolimus for synergistic antipsoriatic efficacy. *Nanomedicine*. 2018;**13**(16):1985-98. [PubMed ID: 30188761]. https://doi.org/10.2217/nnm-2018-0135.
30. Calder PC. Omega-3 fatty acids and inflammatory processes: from molecules to man. *Biochem Soc Trans*. 2017;**45**(5):1105-15. [PubMed ID: 28900017]. https://doi.org/10.1042/ST20160474.
31. Balić A, Vlašić D, Žužul K, Marinović B, Bukvić Mokos Z. Omega-3 versus omega-6 polyunsaturated fatty acids in inflammatory skin diseases. *Int J Mol Sci*. 2020;**21**(3):741. [PubMed ID: 31979308]. [PubMed Central ID: PMC7037798]. https://doi.org/10.3390/ijms21030741.
32. Lorente-Cebrián S, Costa AGV, Navas-Carretero S, Zabala M, Laiglesia LM, Martínez JA, et al. An update on the role of omega-3 fatty acids on inflammatory and degenerative diseases. *J Physiol Biochem*. 2015;**71**(2):341-349. [PubMed ID: 25752887]. https://doi.org/10.1007/s13105-015-0395-y.
33. Sawada Y, Saito-Sasaki N, Nakamura M. Omega-3 fatty acids and skin diseases. *Front Immunol*. 2021;**11**. 623052. [PubMed ID: 33613558]. [PubMed Central ID: PMC7892455]. https://doi.org/10.3389/fimmu.2020.623052.
34. Danaei M, Dehghankhold M, Ataei S, Hasanzadeh Davarani F, Javanmard R, Dokhani A, et al. Impact of particle size and polydispersity index on clinical applications of lipidic nanocarrier systems. *Pharmaceutics*. 2018;**10**(2):57. [PubMed ID: 29783687]. [PubMed Central ID: PMC6027495]. https://doi.org/10.3390/pharmaceutics10020057.
35. Honary S, Zahir F. Effect of zeta potential on the properties of nano-drug delivery systems (Part 2). *Trop J Pharm Res*. 2013;**12**(2):265-73. https://doi.org/10.4314/tjpr.v12i2.20.
36. Higuchi T. Rate of release of medicaments from ointment bases containing drugs in suspension. *J Pharm Sci*. 1961;**50**(10):874-5. [PubMed ID: 13907269]. https://doi.org/10.1002/jps.2600501018.
37. Korsmeyer RW, Gurny R, Doelker E, Buri P, Peppas NA. Mechanisms of solute release from porous hydrophilic polymers. *Int J Pharm*. 1983;**15**(1):25-35. https://doi.org/10.1016/0378-5173(83)90064-9.
38. Dash S, Murthy PN, Nath L, Chowdhury P. Kinetic modeling on drug release from controlled drug delivery systems. *Acta Pol Pharm*. 2010;**67**(3):217-23. [PubMed ID: 20524422].
39. Ng SF, Rouse JJ, Sanderson FD, Meidan V, Eccleston GM. Validation of a static Franz diffusion cell system for in vitro permeation studies. *AAPS PharmSciTech*. 2010;**11**(3):1432-41. [PubMed ID: 20842539]. [PubMed Central ID: PMC2974154]. https://doi.org/10.1208/s12249-010-9522-9.
40. Mohammadi GhanatGhestani M, Sabeti B, Manoochehri S. Preparation and Physicochemical Characterization of Ofloxacin-Loaded Alginate-Chitosan Nanogel: Comparison to Ofloxacin-Loaded Alginate Nanogel. *Jundishapur J Nat Pharm Prod*. 2026;**21**(1). e167048. https://doi.org/10.5812/jjnpp-167048.
41. Németh Z, Csóka I, Semó K, Györke G, Takács-Novák K. Quality by design-driven zeta potential optimisation of nanosuspensions. *Pharmaceutics*. 2022;**14**(9):1897. [PubMed ID: 36145645]. [PubMed Central ID: PMC9505135]. https://doi.org/10.3390/pharmaceutics14091897.
42. Beg S, Rahman M, Kohli K. Quality-by-design approach as a systematic tool for the development of nanopharmaceutical products. *Drug Discov Today*. 2019;**24**(3):717-25. [PubMed ID: 30557651]. https://doi.org/10.1016/j.drudis.2018.12.002.